LINEAR AND NONLINEAR ANALYSIS OF MAGNETIC BEARING BANDWIDTH DUE TO EDDY CURRENT LIMITATIONS

Andrew Kenny
Dr. Alan Palazzolo
Department of Mechanical Engineering
Vibration Control and Electromechanics Laboratory
Texas A&M University
College Station, TX 77840

SUMMARY

Finite element analysis was used to study the bandwidth of alloy hyperco50a and silicon iron laminated rotors and stators in magnetic bearings. A three dimensional model was made of a heteropolar bearing in which all the flux circulated in the plane of the rotor and stator laminate. A three dimensional model of a plate similar to the region of a pole near the gap was also studied with a very fine mesh. Nonlinear time transient solutions for the net flux carried by the plate were compared to steady state time harmonic solutions. Both linear and quasi-nonlinear steady state time harmonic solutions were calculated and compared. The finite element solutions for power loss and flux bandwidth were compared to those determined from classical analytical solutions to Maxwell's equations.

INTRODUCTION

Several commercial finite element codes which solve electromagnetic problems include both a steady state time harmonic solver and a time transient solver. Both of these include the induced eddy currents in the solution. Analysis with a time harmonic solver has the advantage that a single solution predicts the response at given frequency. For a magnetic bearing supporting a shaft running at a steady speed, the time harmonic solver would be the most desirable choice since the time transient solver requires many solutions in the form of time steps for at least one period of the control signal.

The purpose of this study was to determine how much the time harmonic solver's inability to accurately model nonlinear flux saturation would affect the bandwidth and power loss predictions for most cases of magnetic bearing analysis. It was expected that flux saturation might affect the solution in two ways. The first would be due to the concentration of flux near the laminate surfaces due to eddy current skin effect. Second, magnetic bearings generally run with a control flux superposed on a bias flux. Time harmonic solvers can't include the effect of the DC bias flux.

NOMENCLATURE

α = parameter defined by skin depth
δ = skin depth of eddy current
μ = material permeability
σ = material conductivity
ω = frequency in radians per second
d = laminate thickness
B = time varying magnetic flux density
E = time varying electric field intensity
H = time varying magnetic field
$\tilde{H}$ = complex magnitude and phase of time harmonic magnetic field
J_f = time varying free conducting electron current density
$\tilde{J}_f$ = complex magnitude and phase of time harmonic current density

THEORY

Magnetic bearings may be expected to support shafts turning at 120,000 rpm or more. This frequency of 2,000 Hz is low enough that the displacement current term, dD/dt, in Ampere's Law may be neglected. For this reason the four quasistatic Maxwell's equations given by equations 1 to 4 are used to model the induced field and eddy current in magnetic bearings [1].

$$\nabla \times \overline{H} = \overline{J}_f \tag{1}$$

$$\nabla \times \overline{E} = -\frac{\partial \overline{B}}{\partial t} \tag{2}$$

$$\nabla \cdot \overline{B} = 0 \tag{3}$$

$$\nabla \cdot \overline{J}_f = 0 \tag{4}$$

The analysis of eddy currents induced in a laminate by a changing magnetic field begins with the derivation of the diffusion equation [2,3]. This is done by combining the constitutive material laws, $B=\mu H$, and $J_f=\sigma E$, with equations (1) to (4), and then taking the curl of Equation (1) as given by equation (5).

$$\nabla \times \nabla \times \overline{H} = \nabla\left(\nabla \cdot \overline{H}\right) - \nabla^2 \overline{H} = \nabla \times J_f \tag{5}$$

After the substitutions this becomes the diffusion equation given by (6).

$$\nabla^2 \overline{H} = \mu\sigma \frac{\partial \overline{H}}{\partial t} \tag{6}$$

The solution to equation (6) is used to compute the induced eddy currents by using equation (1).

Equations (1) and (2) are intertwined by the material constitutive laws so that in a conductive material, the induced eddy currents cause their own magnetic fields which cancel the original external field and effectively shield deeper material from any magnetic field. The effect is that the magnetic flux and eddy currents are concentrated on the surface . To get a quantitative estimate of this effect in the laminates of magnetic bearings, equation (6) can be solved with the boundary conditions of a flat plate.

Figure 1 shows a conducting laminate in which the magnetic and electric fields are induced by a sinusoidal external magnetic field. The internal field must be the solution to equation (6) reduced to one dimension as shown by equation (7).

$$\frac{\partial^2 H_y}{\partial x^2} = \mu\sigma \frac{\partial H_y}{\partial t} \tag{7}$$

The general solution to equation (7) is equation (8) where H tilde has both a magnitude and phase. The spatial variation of H tilde depends on both the initial conditions and the boundary conditions. For the two sided plate shown in Figure 1 the magnetic field is given by equation (9). It follows from equation (1) that the eddy currents are described by equation (10). Alpha is defined in terms of the skin thickness, delta, as given by equations (10) and (11)

$$H_y = \tilde{H}_y(x) e^{j\omega t} \tag{8}$$

$$\tilde{H}_y(x) = H_o \frac{\cosh(\alpha x)}{\cosh(\alpha d/2)} \tag{9}$$

$$\tilde{J}_z(x) = \alpha H_o \frac{\sinh(\alpha x)}{\cosh(\alpha d/2)} \tag{10}$$

$$\alpha = \frac{1+j}{\delta} \tag{11}$$

$$\delta = \sqrt{\frac{2}{\omega\mu\sigma}}$$

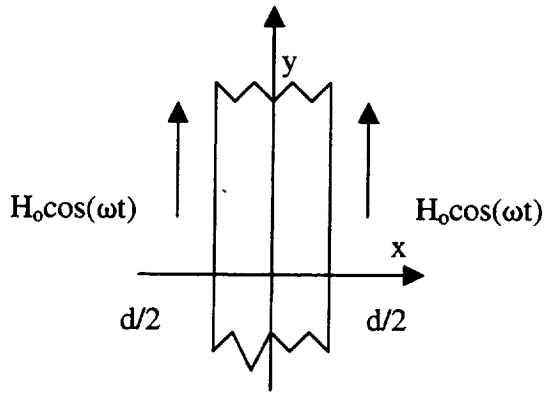

Figure 1. Sketch of Infinite Plate and Magnetic Fields

The eddy current losses per unit area of the laminate can be calculated from the integral given by equation (13). The star indicates complex conjugate. Utilizing the current density distribution given by equation (10) and performing the integration results in the power loss expression of equation (14). A plot of the power loss in a laminate of alloy Hyperco50a is given in Figure 2.

$$P = \frac{1}{2}\int_{-\frac{d}{2}}^{\frac{d}{2}} \frac{\tilde{J}_z \tilde{J}_z^*}{\sigma} dx \tag{13}$$

$$P = \frac{H_o^2}{\sigma\delta}\left[\frac{\sinh\left(\frac{d}{\delta}\right)-\sin\left(\frac{d}{\delta}\right)}{\cosh\left(\frac{d}{\delta}\right)+\cos\left(\frac{d}{\delta}\right)}\right] \tag{14}$$

There are two regions to the curve given by figure (2). For laminates less than about 2 skin depths thick, the eddy currents are too low to cause their own magnetic field and reduce the magnetic field penetrating the conductor. In this region of the curve, the power loss is called resistance limited and is proportional to the cube of the laminate thickness.

For laminates with a ratio of laminate thickness to skin depth of more than four, the field induced by surface eddy currents shields the deeper volume of the laminate from the external field. Since the power loss is reduced by the induced eddy currents on the surface, the power loss for thick laminates is termed inductively limited.

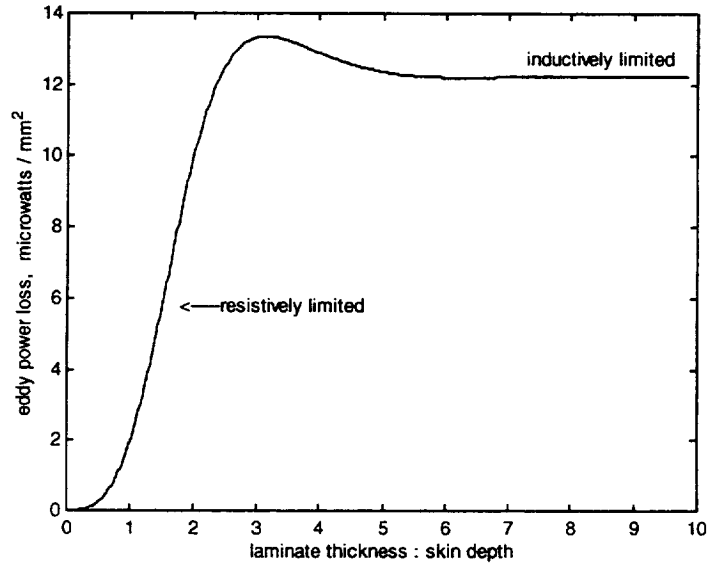

Figure 2. Eddy current loss in Hyperco50a (relative permeability 7500, conductivity 2500 /(ohm*mm)).

FINITE ELEMENT ANALYSIS RESULTS

The eddy current losses in a heteropolar magnetic bearing were analyzed. A bearing of this type is shown in Figure 3. There are several planes of normal and tangential flux symmetry in this bearing. These were taken advantage of to make a finite element model with fewer nodes, finer mesh density, and better aspect ratio. Figure 4 shows the finite element model of the heteropolar bearing used for this study.

The material modeled was a silicon iron with a conductivity of 5500/(ohm-mm) and a relative permeability of 1214. The coil excitation frequency was 100 Hz. At this frequency, the skin depth was .616 mm. The thickness of the laminate was varied from half a skin depth (0.308 mm) to four times the skin depth (1.232 mm). These thicknesses were in the resistive region of the power loss curve, which is where a magnetic bearing would be expected to be operating.

The power loss for the heteropolar bearing includes the stator and rotor laminates. Figure 5 shows the power loss calculated using the steady state ac solver which used a constant relative permeability to calculate the solution. The power loss calculated with the analytical flat plate formula given by equation (14) is shown on the same graph for comparison. The main reason the plots are not the same is that in the heteropolar laminate the value of the magnetic field, Ho, varies. It is less at the outer circumference of the path and higher near the inner corners. Equation (14) indicates the power loss is very sensitive to the chosen level of the field.

In addition to causing power loss, the eddy currents also causes the magnetic flux to lag the control current as evident in equation (9). The force the bearing exerted on the shaft is proportional to the square of the flux in the air gap. The magnitude and phase of the gap flux was determined from the finite element analysis. Since there are no eddy currents in the gap, the magnitude and phase of the flux in the gap is uniform throughout. Figure 6 shows the effect of laminate thickness on gap flux. Better than 99 percent of the maximum obtainable flux in the gap is reached when the laminate has been reduced to two skin thicknesses.

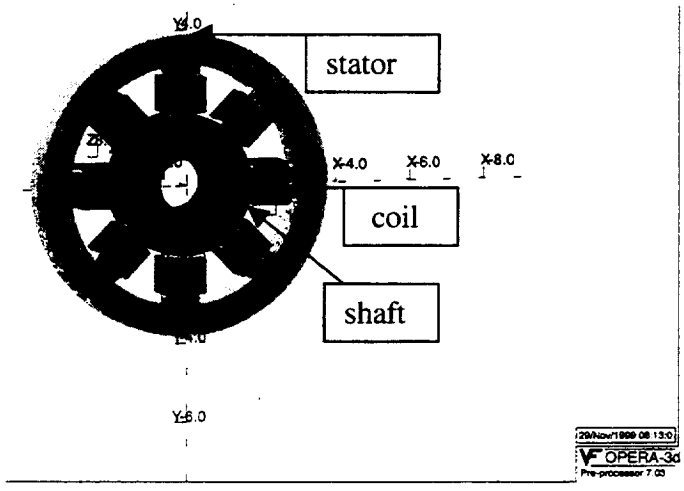

Figure 3. Heteropolar Magnetic Bearing

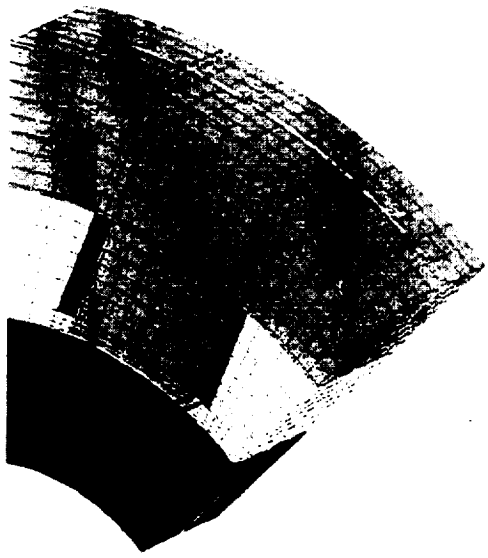

Figure 4. Finite Element Model of Heteropolar Magnetic Bearing. 32000 Nodes, Maximum Element Edge Aspect Ratio 32:1.

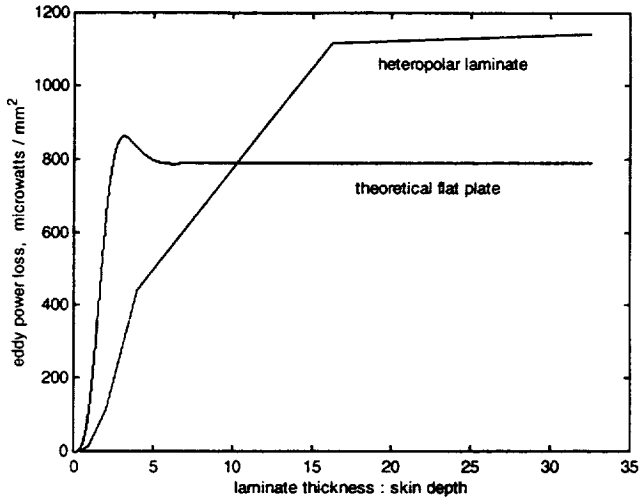

Figure 5. Power Loss in Laminate of Heteropolar Bearing Versus Laminate Thickness. Results of Steady State AC Solver with Constant Relative Permeability. [100 Hz, Peak gap flux .5 T]

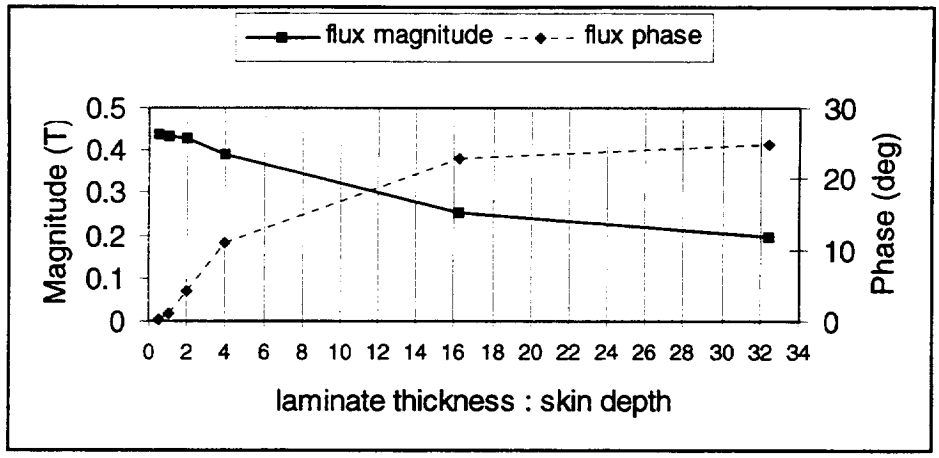

Figure 6. Magnitude and Phase of Flux in Gap of Heteropolar Magnetic Bearing Versus Laminate Thickness.

One of the major motivations for this work was the difficulty in obtaining time transient results using a nonlinear BH curve. For a model as large as that of the heteropolar bearing shown in Figure 4, a linear steady state ac solution could be obtained in a few hours of computer calculation. A time transient model of 64 time steps over two cycles of the control current would take days or weeks. A new model was designed to estimate what the sacrifice in the accuracy of the power loss and flux frequency response would be if the linear steady state ac analysis was performed.

Figure 7 was the new finite element model. It was a plate with zero electrical conductivity butted to a conducting plate. The purpose of this geometry was to transmit an even flux distribution in through the edge of the conducting plate in a similar fashion to flux entering the edge of a stator pole from an air gap.

This model covered a very small area. Each plate is only 5 mm x 5 mm. Only 14000 nodes were needed to model the entire plate with brick elements with an edge length equivalent to the skin depth. For a distance of two skin depths from the plate edges, there were eight elements and the edge length was reduced to one fourth the skin depth for a distance two skin depths. The plate thickness was two skin depths (.734 mm) at 100 Hz with the properties of alloy hyperco50a. Because of symmetry only half the plate thickness needed to be modeled. There were four elements through the half thickness of the model. Therefore, there were four elements through all the outer skin regions. Analyses with successively finer meshes showed this model to produce precise results.

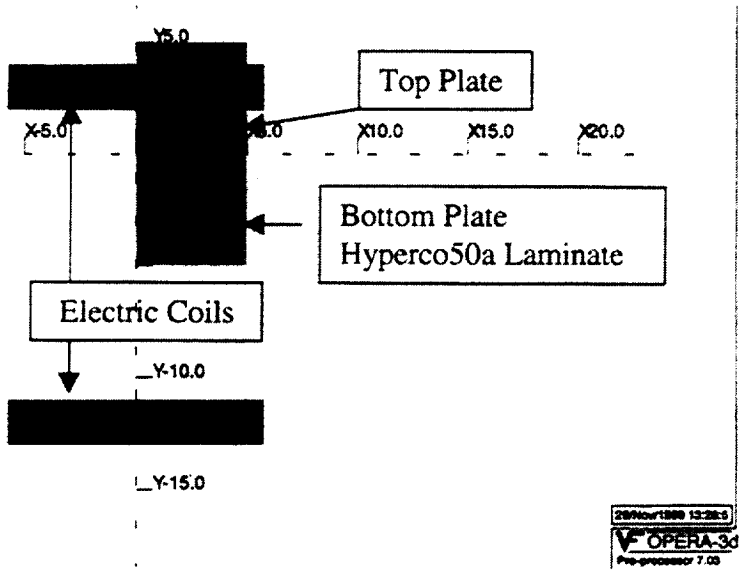

Figure 7. Two Plate, One Fourth Symmetry, Model With Drive Coils.

The power loss and average flux density in the conducting laminate was calculated using three different solvers. First was the steady state linear ac solver, second was the quasi-nonlinear solver, and finally was the time transient nonlinear solver with 50 time steps each equal to one thirty-second of a period of 100 Hz. The quasi-nonlinear solution has the magnetic flux density and magnetic field in phase like similar to the linear solution, but the quasi-nonlinear solver utilizes the nonlinear BH curve and limits the flux from exceeding saturation [4].

The current in the drive coils was set to produce a peak alternating flux of about one tesla. For the steady state analyses this meant the maximum flux was about 1 T and the minimum was –1 T. The time transient analysis included a DC bias flux of 1 T as would be typical in a magnetic bearing. In that case the maximum flux was about 2 T and the minimum about 0 T. Figure 8 shows the nonlinear BH curve used for alloy hyperco50a.

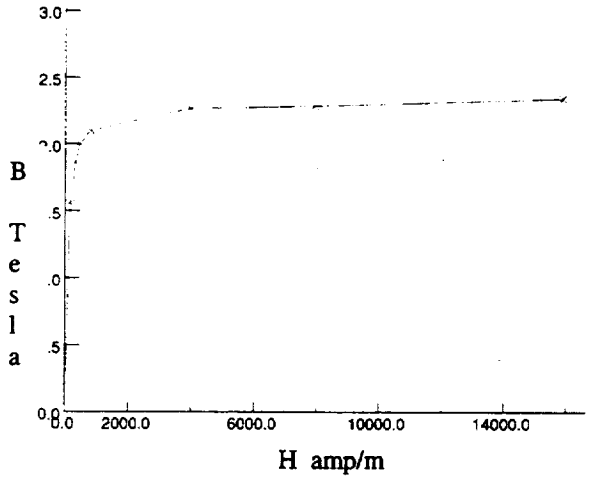

Figure 8. Alloy hyperco50a nonlinear BH curve [5].

A table comparing the energy loss per cycle calculated by each of the three different solvers is shown below. The difference between any of the three solution methods is less than one tenth of one percent. This is especially remarkable considering the plot of the power loss calculated by the nonlinear time transient solution method over one period of the coil current (shown in Figure 9). Although the power loss is only shown over one period of the coil current, further time steps showed these two power loss humps to repeat themselves. The first peak is higher because the flux starts at near zero tesla and reaches a faster rate of change than when the flux decreases from its peak value which is slightly lowered by saturation. The energy loss per cycle was calculated by integrating the area underneath the repeating peaks.

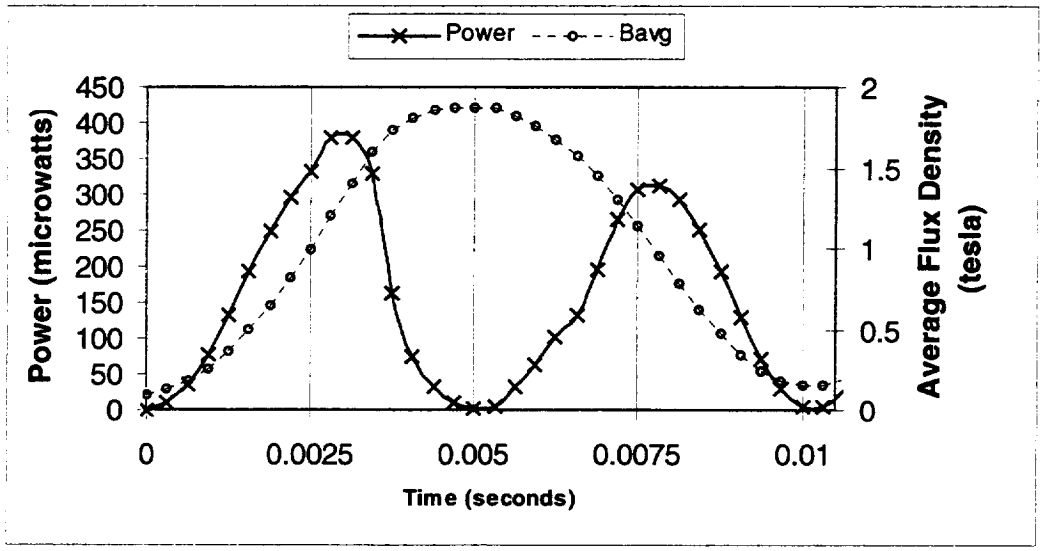

Figure 9. Nonlinear Time Transient Analysis on Two Skin Depth Thick Laminate .

Table 1. Comparison of Eddy Current Energy Loss Per Cycle Computed by Three Methods.

Nonlinear Time Transient	Quasi-nonlinear Steady State	Linear Steady State
1.585 micro Joules	1.579 micro Joules	1.586 micro Joules

Finally the average flux density carried by the conducting plate is shown in the table below as calculated by the three different methods. The average flux density times the plate cross section is the total flux the plate can transport and directly affects the force that can be applied by a laminated heteropolar bearing. Nonlinear saturation reduces the peak flux density calculated by the nonlinear time transient and quasi-nonlinear steady state solvers by 4.6 to 3.2 percent compared to the linear steady state analysis. The phase lag of the average flux density calculated by the time transient analysis varied from zero degrees when increasing to four degrees after peaking and decreasing.

Table 2. Comparison of Average Flux Density Computed by Three Methods. [Magnitude and Phase Lag].

Nonlinear Time Transient	Quasi-nonlinear Steady State	Linear Steady State
.978 T; 0 to 4 degrees	.965 T; 3.69 deg	1.01 T; 3.66 deg

CONCLUSIONS

A laminate of a heteropolar bearing stator and shaft was modeled with three dimensional finite elements. For laminate thicknesses below two skin depths, both the finite element solution and the theoretical assumption showed the power loss to increase as a resistively limited loss. The finite element linear ac analysis showed that better than 99 percent of the maximum obtainable flux in the gap was achieved with laminates two or less skin depths thick.

A fine mesh model was made to simulate a small section of a laminate in a heteropolar bearing. In the skin regions, element edges were just one fourth of a skin depth in length. The power loss calculated by the nonlinear time transient solver was compared to that computed by a linear steady state ac solver and a quasi-nonlinear steady state ac solver. The comparison showed that the power loss predicted by the steady state ac solvers was the same as the average energy loss per cycle predicted by the nonlinear time transient solver. The nonlinear time transient solver and the quasi-nonlinear steady state ac solver predicted peak values of the AC flux magnitude that differed by just 1.3 percent.

ACKNOWLEDGEMENT

The authors gratefully acknowledge the technical and funding support provided by NASA Glenn Space Power and Dynamics Branch (Albert Kascak, Raymond Beach, and Gerold Montague) and the Office of Naval Research – Naval Surface Warfare Center (Tom Calvert, Lyn Peterson, and Glenn Bell).

BIBLIOGRAPHY

[1] Wiley Encyclopedia of Electrical and Electronics Engineering, Volume 6, Eddy Currents, 163-178, Eddy Currents, John Wiley, New York, 1999.

[2] Stoll, R.L., The Analysis of Eddy Currents, Clarendon Press, Oxford, 1974.

[3] Lammeraner J. , Stafle, M., Eddy Currents, CRC Press, 1964.

[4] Opera-3d Users Guide, Chapter 3, Time Variation in Electra, Vector Fields Ltd, Oxford, 1999.

[5] Carpenter Magnetic Alloys, Carpenter Technology Corporation, Carpenter Steel Division, 1995.